Protein epitopes correspond to specific arrangements of amino acid residues, and some such epitopes are contained in short continuous segments of peptide sequences (*18*). Our results show one example of a segmental (continuous) epitope that keeps at least a part of its biological activity when genetically incorporated into the middle of a highly structured membrane protein. To evaluate the generality of the system it will be necessary to study the integration of other sequences into the S gene encoding different epitopes and the variation of the site of insertion into the HBsAg protein.

As previously suggested by Valenzuela *et al.* (*19*), HBsAg particles could be useful as immunogenic carriers of foreign antigens for the preparation of vaccines. Our approach may also be useful for studying the biological activity of other peptides incorporated into the surface of an ordered multimolecular complex. The constitutive expression and secretion of the hybrid envelope particles by established cell lines provide an efficient system for the production of such structures.

REFERENCES AND NOTES

1. P. Tiollais, C. Pourcel, A. Dejean, *Nature (London)* **317**, 489 (1985).
2. D. L. Peterson, D. A. Paul, F. Gavilanes, D. T. Achord, *Advances in Hepatitis Research*, F. V. Chisari, Ed. (Masson, New York, 1984), pp. 30–39.
3. W. Stibbe and W. H. Gehrlich, *J. Virol.* **46**, 626 (1983).
4. A. R. Neurath and S. B. H. Kent, *Immunochemistry of Viruses*, M. H. V. Van Regenmortel and A. R. Neurath, Eds. (Elsevier, New York, 1985), pp. 325–366; D. R. Milich *et al.*, *Science* **228**, 1195 (1985).
5. D. H. Persing, H. E. Varmus, D. Ganem, *Proc. Natl. Acad. Sci. U.S.A.* **82**, 3440 (1985).
6. M. F. Dubois *et al.*, *ibid.* **77**, 4549 (1980); C. Pourcel *et al.*, *J. Virol.* **42**, 100 (1982).
7. A. M. Moriarty *et al.*, *Proc. Natl. Acad. Sci. U.S.A.* **78**, 2606 (1981).
8. P. Valenzuela *et al.*, *Nature (London)* **298**, 347 (1982).
9. F. Delpeyroux *et al.*, in preparation.
10. E. A. Emini, B. A. Jameson, E. Wimmer, *Nature (London)* **304**, 699 (1983).
11. B. Blondel *et al.*, *Virology* **126**, 707 (1983); S. Van der Werf *et al.*, *Proc. Natl. Acad. Sci. U.S.A.* **80**, 5080 (1983); C. Wychowski *et al.*, *EMBO J.* **2**, 2019 (1983).
12. D. L. Peterson, *J. Biol. Chem.* **256**, 6975 (1981).
13. C. E. Fricks, J. P. Icenogle, J. M. Hogle, *J. Virol.* **54**, 856 (1985).
14. F. Delpeyroux, unpublished results.
15. S. van der Werf, unpublished results.
16. R. L. Anacker and J. J. Munoz, *J. Immunol.* **87**, 426 (1961).
17. J. M. Hogle, M. Chow, D. J. Filman, *Science* **229**, 1358 (1985).
18. J. A. Berzofsky, *ibid.* **229**, 932 (1985); M. H. V. Van Regenmortel and A. R. Neurath, *Immunochemistry of Viruses*, M. H. V. Van Regenmortel and A. R. Neurath, Eds. (Elsevier, New York, 1985), pp. 1–11; J. G. Sutcliffe, T. M. Shinnick, N. Green, R. A. Lerner, *Science* **219**, 660 (1983).
19. P. Valenzuela *et al.*, *Bio/Technology* **3**, 323 (1985).
20. M. Lusky and M. Botchan, *Nature (London)* **293**, 79 (1981).
21. F. L. Graham and A. J. Van der Eb, *Virology* **52**, 456 (1973); M. Wigler *et al.*, *Proc. Natl. Acad. Sci. U.S.A.* **76**, 1373 (1979).
22. F. Colbère-Garapin, F. Horodniceanu, P. Kourilsky, A. C. Garapin, *J. Mol. Biol.* **150**, 1 (1981).
23. M. L. Michel *et al.*, *Proc. Natl. Acad. Sci. U.S.A.* **81**, 7708 (1984).
24. U. K. Laemmli, *Nature (London)* **227**, 680 (1970).
25. P. Couillin *et al.*, *Ann. Virol. (Inst. Pasteur)* **133E**, 315 (1982).
26. A. Voller, D. E. Bedwell, A. Berlett, *A Guide with Abstracts of Microplate Applications* (Dynatech, Guernesey, 1979), p. 1.
27. B. Blondel *et al.*, *J. Virol.* **57**, 81 (1986).

28. We thank C. Gouyette for oligonucleotide synthesis, M. C. Prévost for electron microscopy, M. O. Mercereau-Puijalon for a helpful suggestion, S. Cole and F. Horaud for critical reading of the manuscript, and C. Turcat for typing. Work in B.B.'s and R.C.'s laboratory was supported by INSERM (83.3008). We dedicated this report to the memory of Y. Malpièce, who died in October 1985.

26 February 1986; accepted 5 May 1986

Calcium and Sodium Channels in Spontaneously Contracting Vascular Muscle Cells

MICHAEL STUREK AND KENT HERMSMEYER*

Electrophysiological recordings of inward currents from whole cells showed that vascular muscle cells have one type of sodium channel and two types of calcium channels. One of the calcium channels, the transient calcium channel, was activated by small depolarizations but then rapidly inactivated. It was equally permeable to calcium and barium and was blocked by cadmium, but not by tetrodotoxin. The other type, the sustained calcium channel, was activated by larger depolarizations, but inactivated very little; it was more permeable to barium than calcium. The sustained calcium channel was more sensitive to block by cadmium than the transient channel, but also was not blocked by tetrodotoxin. The sodium channel inactivated 15 times more rapidly than the transient calcium channel and at more negative voltages. This sodium channel, which is unusual because it is only blocked by a very high (60 μM) tetrodotoxin concentration but not by cadmium, is the first to be characterized in vascular muscle, and together with the two calcium channels, provides a basis for different patterns of excitation in vascular muscles.

ELECTRICAL EXCITATION OF VASCULAR muscles is characterized by a range of depolarization patterns that includes responses with unusually rapid onset and very long duration (*1*). Electrical spikes of a typical spontaneously active vascular muscle cell cause phasic contraction, while sustained depolarization causes tonic contraction (*1, 2*). These diverse forms of activation may be due to differential activation of various ion channels. Because vascular muscle excitation is likely to be calcium dependent (*1–3*), and because multiple types of calcium channels exist in other cell types (*4*), vascular muscle cells might be expected to have several types of calcium channels. The presence of sodium channels might provide additional combinations of inward current in these cells.

Voltage clamp data that could characterize different ion channels in vascular muscle have been technically difficult to obtain until the development of tight-seal pipette recording (*5*). With tight-seal recording from whole cells (*6*), we determined the voltage-dependent, inward-current channels in vascular muscle cells that might distinguish them from other cell types. For our studies, we used isolated, single vascular muscle cells that have been characterized electrophysiologically and pharmacologically (*7*). We did not use subcultured cell lines because they lose membrane excitability, pharmacological identity, and the ability to contract (*8*). Rather, we did all of our experiments with primary cultures of azygos venous muscle cells from neonatal rats (*9*); these vascular muscle cells contract spontaneously and show membrane properties (for example, 50 mV spikes and −45 mV resting potentials) appropriate for the blood vessel from which they were isolated (*7*).

Vascular muscle cells were studied in solutions that suppress outward potassium currents; cesium and EGTA were included in the recording electrode solution and barium and tetraethylammonium (TEA) were included in the external solution (*10*). For Na^+ current, only half of the Na^+ was replaced by TEA in extracellular solutions. Calcium currents were studied only after external sodium chloride was completely replaced by TEA chloride to characterize the smaller Ca^{2+} currents (Fig. 1, A and B).

Voltage clamp analysis in Na^+-containing

Department of Pharmacology, Cardiovascular Center, University of Iowa, Iowa City, IA 52242.

*To whom requests for reprints should be addressed.

Table 1. Characteristics of vascular muscle inward currents. The holding potential for transient calcium current (I_{Ca}) and sodium current (I_{Na}) was always −80 mV and for the sustained I_{Ca} was always −30 mV. Decay $t_{1/2}$ was the time (in milliseconds) for decay of the 0 mV current to half of its peak value. Fractional current (I) for both TTX and cadmium conditions was the peak current after exposure to the particular agent divided by the peak current in the control condition, thus giving the relative current remaining. I_{Ba}/I_{Ca} is the ratio of the peak Ba^{2+} current (I_{Ba}) in Ba20s to the peak Ca^{2+} current (I_{Ca}) in Ca20s external solution. Ca20c was used for each I_{Na} measurement and Ca20s for each I_{Ca} measurement. See (*10*) for solution composition. The probability level chosen for statistically significant difference was $P < 0.05$. Statistical analysis for the decay $t_{1/2}$ from depolarizations to 0 mV and TTX blockade consisted of a one-way analysis of variance and Sheffe post hoc test. Statistical analysis for the cadmium ($CdCl_2$) blockade and I_{Ba}/I_{Ca} ratio was a *t* test for independent groups. Values are mean ± SEM; number of cells are in parentheses.

Current	Decay $t_{1/2}$ (msec)	Fractional I		I_{Ba}/I_{Ca}
		60 μ*M* TTX	100 μ*M* $CdCl_2$	
Transient I_{Ca}	13* ± 1 (28)	1.03† ± 0.05 (6)	0.60‡ ± 0.05 (3)	0.94‡ ± 0.02 (6)
Sustained I_{Ca}	227* ± 26 (21)	0.94† ± 0.07 (6)	0.35‡ ± 0.08 (3)	3.81‡ ± 0.26 (6)
I_{Na}	0.9* ± 0.1 (7)	0.03 ± 0.02 (5)	0.92 ± 0.03 (4)	—

*All three current groups were significantly different from each other. †Significantly different from I_{Na}; ‡Significantly different transient and sustained divalent cation currents.

solution revealed a prominent Na^+ current in each vascular muscle cell. The average Na^+ current peaked within 0.7 msec, decayed to half of the 3-nA peak amplitude in 0.9 msec, and decayed almost to zero after 10 msec, leaving only a smaller divalent current (Fig. 1B). This is probably the only type of Na^+ current in these cells because eliminating Na^+ from the extracellular solution (*10*) did not increase membrane resistance. Input resistance measured by a small, hyperpolarizing current pulse was 3.6 ± 1.7 (SEM) gigaohms in Na^+-containing solution and 2.6 ± 0.4 gigaohms in Na^+-free solution. The Na^+-dependent current was reduced by 50 percent by 30 μ*M* tetrodotoxin (TTX) and blocked entirely by 60 μ*M* TTX. Thus, the Na^+ channel currents in vascular muscle appear to differ in TTX sensitivity from those reported in cardiac muscle or neurons (*11*). However, the Na^+ channel was blocked less than 10 percent by 100 or 500 μ*M* cadmium.

In Na^+-free solution, two types of Ca^{2+} currents were apparent in vascular muscle cells when we examined their inactivation kinetics, voltage dependence, permeability to Ba^{2+}, and sensitivity to block by cadmium. We generated a family of current traces from a single cell by step depolarization to +10 mV from holding potentials that ranged from −80 to 0 mV in Na^+-free solution with 10 m*M* Ca^{2+} present (Fig. 1A). There was a qualitative difference in the first 50 msec of the inward currents depending on whether the holding potentials were positive or negative to −30 mV. Step depolarizations to +10 mV from holding potentials ranging from −80 to −40 mV triggered an early transient current followed by a sustained plateau; step depolarizations to +10 mV from −30 to 0 mV showed only the sustained plateau phase. The average time for the sustained Ca^{2+} current to decay to half of peak amplitude (decay to $t_{1/2}$) was 17 times longer than that of the transient current at 0 mV (Table 1). Activation rates of all currents were identical in the early phase, as shown by the superimposed traces (Fig. 1A), but differences in inactivation of the currents and the abrupt −30 mV transition point suggested that there were two components of the Ca^{2+} current. We have referred to these as the transient and sustained Ca^{2+} channels.

The Ca^{2+} currents could be separated because the two channels inactivated at different membrane potentials (holding potential). We subtracted (digitally) the sustained current from the total current and determined that the transient current completely decayed to zero within 75 msec (Fig. 1A). We used depolarization to +10 mV from holding potentials of −30 and −80 mV to determine that 146 of the 153 spontaneously contracting cells had both components (transient and sustained) of the Ca^{2+} current; six of the remaining seven cells had only sustained current and one cell had only transient current. The transient Ca^{2+} current was predominant in most cells, accounting for 92 percent of the current from the most negative holding potential of −80 mV. However, at holding potentials near resting potential (−45 mV), more than half of the transient Ca^{2+} channels were inactivated; in contrast, all sustained channels were available for activation at membrane potentials negative to −20 mV, and only half of the channels were inactivated if the cell were depolarized to −7 mV (Fig. 1C).

The existence of two different Ca^{2+} channels was supported by Ba^{2+} replacement experiments. Sustained current was 3.8 times greater when Ba^{2+} replaced Ca^{2+} as the external charge carrier. In contrast, the transient current was the same if Ca^{2+} or Ba^{2+} was present in the bathing solution (Table 1). Therefore, the sustained channel is more permeable to Ba^{2+} than to Ca^{2+}, whereas the transient channel is equally permeable to both divalent cations. To test the independence of the two channels we determined their susceptibility to blockade by the divalent cation cadmium. Cadmium [100 μ*M*, in Ca20s extracellular solution (*10*)]

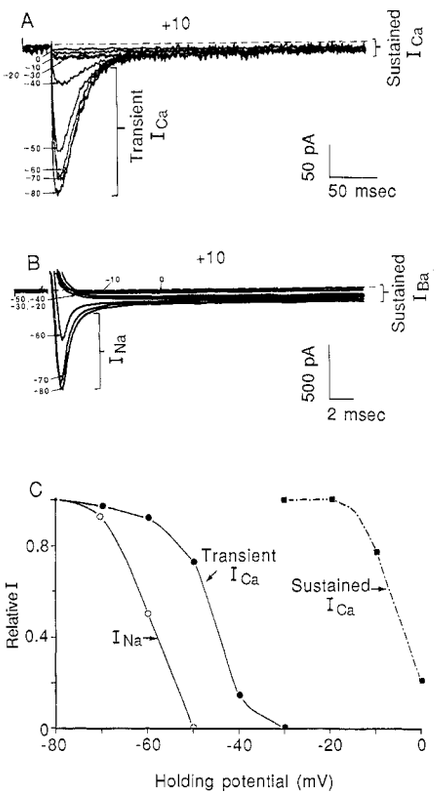

Fig. 1. Inactivation of calcium currents in a typical single cell. (A) A family of Ca^{2+} current traces resulting from depolarization to +10 mV from holding potentials ranging from −80 mV to 0 mV in 10 mV increments (indicated to the left of the traces) (Ca10s). Holding potentials were established for 5 to 10 seconds to reach a quasi steady state, followed by depolarization to the test potential (+10 mV) for 350 msec. The dashed line represents the zero current level in this and subsequent figures. Transient and sustained portions of the calcium current (I_{Ca}) are labeled. All currents have been corrected for leakage and capacitance. (B) A family of Na^+ and Ca^{2+} channel currents resulting from depolarization to +10 mV from holding potentials ranging from −80 mV to 0 mV (indicated to the left of the traces) (Ba20c). This cell shows only sustained divalent channel current (I_{Ba}), which is labeled to contrast with I_{Na}. Note the different time scale and current scale from (A). Currents did not require correction for leakage and capacitance. (C) Inactivation analysis of Ca^{2+} and Na^+ currents. These curves represent plots of peak currents shown in (A) and (B). Sustained I_{Ca} is that current elicited by pulses from holding potentials (V_H) of −30, −20, −10, or 0 mV and plotted relative to the maximum sustained I_{Ca} (from the test pulse of −30 mV). Transient I_{Ca} (isolated by the subtraction technique described in the text) is plotted relative to maximum transient I_{Ca} from the −80 mV test pulse. Curves were fitted by eye.

decreased the transient Ca^{2+} current significantly less than it did the sustained Ca^{2+} current (Table 1). At 500 μM cadmium, both Ca^{2+} channels were blocked by more than 98 percent. Neither Ca^{2+} current could be attributed to Ca^{2+} movement through the Na^+ channel, as indicated by the lack of any block of the Ca^{2+} currents by TTX (Table 1). Both the differential permeability and the blockade of the Ca^{2+} currents further indicate that there are two distinct types of Ca^{2+} channels and not a single type of channel that exists in two different states.

We compared the Ca^{2+} channel currents to the Na^+ current of another cell (Fig. 1B). This cell was chosen because the large amplitude (124 pA) of the sustained divalent-ion (Ba^{2+}) current allowed comparison of the time courses of the two currents. Peak Na^+ current was seven times larger than peak sustained Ba^{2+} current, and the decay $t_{1/2}$ of the Na^+ current (0.9 msec) was less than 1/15th of the decay $t_{1/2}$ of the transient Ca^{2+} current (Table 1). The different time courses of both activation and inactivation of the Na^+ current are compared to the sustained Ba^{2+} current (Fig. 1B). Complete, steady-state inactivation of the Na^+ channel occurred at -50 mV (Fig. 1C), compared to -30 mV and above 0 mV for the transient and sustained Ca^{2+} currents, respectively.

To further separate the two distinct Ca^{2+} channels, we conducted current-voltage analyses using depolarizations to different step potentials from constant holding potentials of -80 or -30 mV, which we had determined would allow full activation of the transient and sustained channels, respectively. Activation occurred in two voltage ranges (Fig. 2). The threshold for activation of the transient channel was -40 mV, maximum current was at -8 mV, and current was not detectable at $+50$ mV and above (Fig. 2, A, B, and E). Activation of the sustained channel was minimal at -10 mV, peaked at about $+40$ to $+50$ mV, and was not detectable at $+70$ mV (Fig. 2, C, D, and E). At more positive potentials, even the sustained current showed a more rapid decline from the peak during a test pulse, indicating inactivation, but never reached zero during the test pulse. The large amplitude of the transient current, which averaged over 100 pA, dominated the Ca^{2+} currents at negative test potentials (Fig. 2E). These large transient Ca^{2+} currents were more than six times as large as the sustained Ca^{2+} currents at a test potential of 0 mV. Both Ca^{2+} channels appeared to exclude all Na^+ at 10 or 20 mM Ca^{2+} concentrations, but exclusion of Na^+ was dependent on external Ca^{2+} (*12*).

Thus, this vascular muscle, in which Ca^{2+} channels are considered the most important

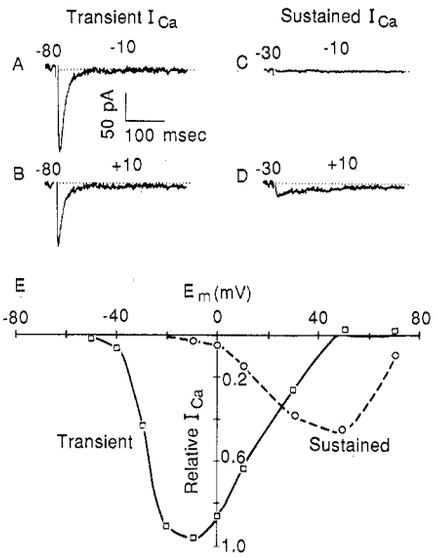

Fig. 2. Separation of the activation voltage ranges for transient and sustained calcium currents (I_{Ca}). Peak inward current was obtained by test pulses to the indicated membrane potentials (E_m) from holding potentials of -80 mV and -30 mV that apparently represent maximum amplitudes of the transient and sustained channels, respectively. Transient I_{Ca} was obtained by subtraction, as described in the text. (A–D) Current tracings for the two types of current from the two different holding potentials elicited by test pulses to -10 mV and $+10$ mV. (E) Activation analysis shows separate current-voltage curves for transient and sustained I_{Ca}. Currents are expressed on a relative scale, as in Fig. 1 (Ca20s).

for membrane excitation (*1–3, 13*), has two types of Ca^{2+} channels and a Na^+ channel. These Ca^{2+} channels are similar in voltage ranges and kinetics to those characterized in neurons, cardiac muscle, and other cell types (*4*). We have also found two types of Ca^{2+} channels in freshly dispersed muscle cells from mesenteric arteries of adult rats (*14*). The distinct feature of Ca^{2+} currents in the spontaneously contracting venous muscle cells used here is the large transient current that predominates over sustained current. The transient current was found in more than 90 percent of these cells, while, for example, only 20 percent of dorsal root ganglion cells had transient current (*4*). In addition, the ratio of transient to sustained current upon depolarization to 0 mV was 6:1 for vascular muscle cells, in comparison to almost an inverse ratio for dorsal root ganglion cells (*4*) or atrial myocardial cells (*15*). The predominance of the transient current may relate to the pacemaking function of these vascular muscle cells in young rats. Finally, the absolute current density in 10 mM Ca^{2+} of 5 pA per picofarad of cell membrane in these cells is the largest of which we are aware.

If the transient Ca^{2+} channel supplies depolarizing current for the upstroke of the electrical spike in these cells, what is the role of the Na^+ channel? The Na^+ channel, together with transient Ca^{2+} channels, may contribute to pacemaking. Although the Na^+ channels are largely inactivated at normal resting membrane potential, they could allow augmented excitation of hyperpolarized cells. The activity of the transient Ca^{2+} channel and Na^+ channel between -60 and -40 mV may reflect the notable pacemaker function and rapid contraction of vascular muscle of azygos vein; this function may be similar to that of the vascular muscle cells that cause pacemaker activity in small arteries (*3*).

Sustained Ca^{2+} channels probably supply Ca^{2+} for contractile protein activation and intracellular storage sites, replacing the continuous loss of intracellular Ca^{2+} (*16*). The magnitude of the sustained influx of Ca^{2+} would be modulated by neurotransmitters, and thus alter contraction amplitude (*17*). Thus, different types and ratios of Ca^{2+} and Na^+ channels may be present in various blood vessels and account for their individual excitation characteristics, as well as their possible differential sensitivities to therapeutic agents.

REFERENCES AND NOTES

1. K. Hermsmeyer, *Life Sci.* **10**, 223 (1971); *Experientia* **35**, 1599 (1979); A. J. Trapani *et al.*, *Eur. J. Pharmacol.* **72**, 87 (1981); K. Hermsmeyer *et al.*, in *Vasodilatation*, P. M. Vanhoutte and I. Leusen, Eds. (Raven, New York, 1981), pp. 273–284; K. Hermsmeyer, *Physiologist* **25**, 454 (1982).
2. K. Hermsmeyer, *Circ. Res.* **33**, 244 (1973).
3. B. Johansson and A. P. Somlyo, in *Handbook of Physiology*, Section 2, *The Cardiovascular System*, D. F. Bohr, A. P. Somlyo, H. V. Sparks, Jr., Eds. (American Physiological Society, Bethesda, MD, 1980), pp. 301–323.
4. B. P. Bean, *J. Gen. Physiol.* **86**, 1 (1985); C. M. Armstrong and D. R. Matteson, *Science* **227**, 65 (1985); J. W. Deitmer, *J. Physiol. (London)* **355**, 137 (1984); S. A. Fedulova, P. G. Kostyuk, N. S. Veselovsky, *ibid.* **359**, 431 (1985); B. Nilius, P. Hess, J. B. Lansman, R. W. Tsien, *Nature (London)* **316**, 443 (1985); M. C. Nowycky, A. P. Fox, R. W. Tsien, *ibid.*, p. 440.
5. B. Sakmann and E. Neher, in *Single Channel Recording* (Plenum, New York, 1983); *Annu. Rev. Physiol.* **46**, 455 (1983).
6. O. P. Hamill, A. Marty, E. Neher, B. Sakmann, F. J. Sigworth, *Pfluegers Arch.* **391**, 85 (1981).
7. K. Hermsmeyer and R. Mason, *Circ. Res.* **50**, 627 (1982); K. Hermsmeyer, *Experientia* **35**, 1599 (1979); W. J. Marvin, Jr., R. B. Robinson, K. Hermsmeyer, *Circ. Res.* **45**, 528 (1979).
8. M. Friedman, G. Kaczorowski, R. Vandlen, G. Katz, J. P. Reuben, *Fed. Proc. Fed. Am. Soc. Exp. Biol.* **44**, 452 (1985); P. Hess *et al.*, *J. Gen. Physiol.* **86**, 5a (1985).
9. We used isolated, single cells in primary cultures of vascular muscle cells. Azygos veins of 15 to 20 decapitated neonatal (1 to 4 days old) rats from the Kyoto-Wistar normotensive (WKY) strain were excised and placed in CV3M, which consists of 4 mM L-glutamine, gentamicin (20 μg/ml), 20 mM Hepes buffer (*p*H 7.3), and 16 mM $NaHCO_3$ dissolved in 85% minimum essential medium–Earle's salts and 15% horse serum. After a rinse in CV3M, the tissue was soaked for 10 minutes in KG solution, consisting of 140 mM potassium glutamate, 25 mM Hepes (*p*H 7.3), 16 mM $NaHCO_3$, 0.5 mM NaH_2PO_4, 16.5 mM dextrose, and 0.014 mM phenol red. The veins were then minced with fine dissecting scissors.

Venous fragments were incubated at 37°C with collagenase (30 mg in 10 ml of KG solution) for 30 minutes. The collagenase supernatant was discarded and the tissue was exposed to three or four 15-minute incubations in 15 ml of trypsin (1 mg/ml) in KG solution. After each incubation, the supernatant was removed and placed in 10 ml of horse serum on ice. The combined supernatant fractions were then centrifuged for 15 minutes at 200*g*, washed by suspension in CV3M, and centrifuged at 200*g* for 5 minutes. The cell pellets were resuspended in 10 ml of CV3M plus 5 μ*M* 5-bromo-2′-deoxyuridine (BrdU) and sedimented in a 15-ml tissue culture flask. The muscle cells were resuspended in CV3M plus BrdU, diluted to a density of 60,000 to 70,000 cells per milliliter, and plated on poly-L-lysine–coated glass cover slips. Cells were grown in a 5% CO_2 incubator at 95% humidity and 37°C.

10. For voltage clamp analysis of inward currents, cells were placed in a perfusion chamber containing a solution (Ca10s) that contained 10 m*M* $CaCl_2$, 135 m*M* TEACl, 1 m*M* $MgCl_2$, 10 m*M* glucose, 10 m*M* Hepes, *p*H adjusted to 7.4 with TEAOH, or a Na^+-containing solution (Ca20c) which was exactly the same, except that $CaCl_2$ was 20 m*M* and TEACl and NaCl were each 67.5 m*M*. Barium was substituted for Ca^{2+} in some cases; the solutions were Ba20s, which contained 20 m*M* $BaCl_2$, 135 m*M* TEACl, 1 m*M* $MgCl_2$, 10 m*M* glucose, and 10 m*M* Hepes (*p*H 7.4), or Ba20c, which contained 20 m*M* $BaCl_2$, 67.5 m*M* TEACl, 67.5 m*M* NaCl, 1 m*M* $MgCl_2$, 10 m*M* glucose, and 10 m*M* Hepes (*p*H 7.4). The pipette solution (PEG 10) consisted of 150 m*M* cesium (Cs) glutamate, 10 m*M* CsEGTA, 5 m*M* $MgCl_2$, and 10 m*M* Hepes (*p*H adjusted to 7.4 with CsOH). After a gigaseal ($\geq 10^9$ ohms) was formed and the cell membrane at the pipette tip ruptured by suction to allow whole cell voltage clamp, ionic currents were recorded. Calcium or Na^+ currents were elicited by 350-msec depolarizations at intervals of 10 to 15 seconds. The currents were amplified by a List EPC-7 amplifier with 0.5-gigaohm feedback resistor and low-pass filtered at 500 Hz. This cutoff, chosen to optimize signal to noise ratio, would have caused an underestimate of Na^+ channel current amplitudes. All data were digitized (the sampling rate was 5000 per second) and stored on floppy disks to permit further analysis. Leak and capacitive currents were subtracted for each record by summation of currents during depolarizing pulses with linearly scaled current elicited in the same cell by 10-mV hyperpolarizing pulses.

11. A. B. Cachelin, J. E. De Peyer, S. Kokubun, H. Reuter, *J. Physiol. (London)* **340**, 389 (1983); C. J. Cohen, B. P. Bean, T. J. Colatsky, R. W. Tsien, *J. Gen. Physiol.* **78**, 383 (1981); R. Horn, J. Patlak, C. F. Stevens, *Nature (London)* **291**, 426 (1981).
12. M. Sturek and K. Hermsmeyer, unpublished observations.
13. K. Hermsmeyer and C. Kuthe, *J. Cardiovasc. Pharmacol.* **6**, 5933 (1984); K. Hermsmeyer and M. Sturek, *ibid.*, in press; C. van Breemen, P. Aaronson, R. Loutzenhiser, *Pharmacol. Rev.* **30**, 167 (1979).
14. B. P. Bean, M. Sturek, A. Puga, K. Hermsmeyer, *Circ. Res.*, in press.
15. B. P. Bean, *J. Gen. Physiol.* **86**, 1 (1985).
16. C. van Breemen, P. Aaronson, R. Loutzenhiser, *Pharmacol. Rev.* **30**, 167 (1979); G. B. Weiss, *Adv. Gen. Cell. Pharmacol.* **2**, 71 (1977); K. Hermsmeyer and M. Sturek, *J. Cardiovasc. Pharmacol.*, in press.
17. H. Reuter, *Nature (London)* **301**, 569 (1983).

18. Supported by grants HL 16328 and HL 32295 from the National Institutes of Health.

14 January 1986; accepted 22 May 1986

Engineering Herbicide Tolerance in Transgenic Plants

DILIP M. SHAH,* ROBERT B. HORSCH, HARRY J. KLEE, GANESH M. KISHORE, JILL A. WINTER, NILGUN E. TUMER, CATHY M. HIRONAKA, PATRICIA R. SANDERS, CHARLES S. GASSER, SERDAR AYKENT, NED R. SIEGEL, STEPHEN G. ROGERS, ROBERT T. FRALEY

The herbicide glyphosate is a potent inhibitor of the enzyme 5-enolpyruvylshikimate-3-phosphate (EPSP) synthase in higher plants. A complementary DNA (cDNA) clone encoding EPSP synthase was isolated from a complementary DNA library of a glyphosate-tolerant *Petunia hybrida* cell line (MP4-G) that overproduces the enzyme. This cell line was shown to overproduce EPSP synthase messenger RNA as a result of a 20-fold amplification of the gene. A chimeric EPSP synthase gene was constructed with the use of the cauliflower mosaic virus 35*S* promoter to attain high level expression of EPSP synthase and introduced into petunia cells. Transformed petunia cells as well as regenerated transgenic plants were tolerant to glyphosate.

GLYPHOSATE IS A POTENT, BROAD-spectrum herbicide that inhibits the growth of both weed and crop species. Glyphosate (*N*-[phosphonomethyl] glycine) interferes with aromatic amino acid biosynthesis by inhibiting the enzyme 5-enolpyruvylshikimate-3-phosphate (EPSP) synthase of the shikimate pathway (*1*–*4*). Inhibition of this enzyme prevents the synthesis of chorismate-derived aromatic amino acids and secondary metabolites in plants.

Glyphosate-tolerant plant cell cultures containing elevated levels of EPSP synthase activity have been reported (*4*, *5*). We have recently described a glyphosate-tolerant *Petunia hybrida* cell line (MP4-G) which was established after stepwise selection on increasing amounts of glyphosate (*6*). This cell line overproduces EPSP synthase 15- to 20-fold. In this study, we have determined that the molecular basis for glyphosate tolerance in the MP4-G cell line is the amplification of the EPSP synthase gene and demonstrate that a chimeric EPSP synthase gene, designed to overproduce EPSP synthase, confers tolerance to glyphosate in transformed petunia calli and in regenerated transgenic plants.

A homogeneous preparation of EPSP synthase (M_r, 49,000 to 55,800) was obtained from the glyphosate-tolerant MP4-G cell line (*6*). Gas-phase microsequencing (*7*) of the purified enzyme yielded a partial amino acid sequence from its NH_2-terminus. Three families of oligonucleotides (EPSP1, EPSP2, and EPSP3) were synthesized, based on codons specifying amino acid residues 8 to 13 (Fig. 1). To facilitate screening of the MP4-G complement DNA (cDNA) library, we determined which of the three families of oligonucleotides contained the correct EPSP synthase messenger RNA (mRNA) sequence. Northern blots containing polyadenylated [poly(A)$^+$] RNA's isolated from the glyphosate-sensitive MP4 cell line and the glyphosate-tolerant MP4-G cell line were hybridized with the oligonucleotide probes. Of the three oligonucleotide probes, only EPSP1 hybridized strongly to a transcript of 1.9 kb that was present in the MP4-G RNA but not in the MP4 RNA. This result suggested that the MP4-G cell line overproduces EPSP synthase mRNA and that EPSP1 contains the correct sequence of EPSP synthase mRNA.

A λgt10 cDNA library was constructed from poly(A)$^+$ RNA isolated from MP4-G cells and was screened with the EPSP1 probe. After three cycles of screening, six phage containing DNA hybridizing to the oligonucleotide probe were isolated. These phage contained cDNA inserts ranging from 180 to 330 bp—a size significantly shorter than the 1.9-kb EPSP synthase mRNA. The 330-bp fragment from one of these cDNA clones was recloned into pUC9 (pMON9531) and sequenced. The amino acid sequence deduced from the nucleotide sequence was identical to that obtained by protein sequencing (*8*). It also revealed that the enzyme was translated as a precursor polypeptide containing a transit peptide of 72 amino acids at the NH_2-terminal end (Fig. 2). A genomic clone containing a 20-kb Bam HI fragment that hybridizes to pMON9531 was isolated from a genomic library of MP4-G DNA. Restriction mapping and DNA sequencing indicated that a 4.6-kb subfragment of this clone contained sequences 3′ of the original cDNA clone. This fragment was then used as a probe to rescreen the cDNA library. Two clones con-

Plant Molecular Biology, Division of Biological Sciences, Monsanto Company, 700 Chesterfield Village Parkway, St. Louis, MO 63198.

*To whom correspondence should be addressed.